

Vibrational Trapping and Suppression of Dissociation in Intense Laser Fields

A. Giusti-Suzor⁽¹⁾ and F. H. Mies⁽²⁾

⁽¹⁾Laboratoire de Chimie-Physique, 11 rue Pierre et Marie Curie, 75231, Paris, France
and Laboratoire de Photophysique Moléculaire, Université Paris-Sud, Orsay, France

⁽²⁾National Institute of Standards and Technology, Gaithersburg, Maryland 20899

(Received 6 December 1991)

We calculate the dissociation of H_2^+ in intense short pulsed laser fields for a variety of wavelengths and a wide range of initial vibrational states ($v=0-14$). While the low- v levels achieve 100% dissociation in the leading edge of the pulse, for high v there is an onset of stabilization, and significant [(5-50)%] population remains in bound vibrational states throughout the entire pulse. The dissociation is incomplete, and a coherent distribution of excited vibrational states is formed. This survival effect can be attributed to the trapping of *portions* of the initial vibrational wave packet in transient laser-induced potential wells.

PACS numbers: 33.80.Gj, 33.80.Wz, 34.50.Rk

Starting from some initial stable state of a diatomic molecule, and given an intense pulsed laser with peak intensity I_p , we might expect that the intensity in the rising edge of the pulse could be sufficient to completely dissociate the molecule well before I_p is reached. Hence no bound-state population will ever experience the peak intensity much less survive to the end of the pulse. Comparable leading-edge saturation effects have been postulated for photoionization [1] and have obfuscated the observation of the strong-field effects associated with the peak intensity. Obviously, for a given I_p , the onset of this saturation effect depends on the photon frequency ω and the duration T_p of the pulse. One might also expect that increasing the initial vibrational level of the molecule v would enhance the early depletion of bound-state population by making the dissociative "bond-softening" effect [2] accessible at lower intensities. Indeed for lower- v states this supposition is nicely confirmed by our calculations for the following process [3]:



As seen in Fig. 1(a) for $\lambda=248$ nm photons and $I_p=5 \times 10^{14}$ W/cm² the $v=0, 1, 2,$ and 3 states progressively undergo 100% dissociation at earlier and earlier stages of the laser pulse which peaks at 41 fs. However, beginning at $v=4$, and for all higher v shown in Fig. 1(b) we observe a remarkable survival of the bound-state population of this intense field.

This stabilization effect is the principal concern of this Letter. A brief examination of Fig. 2, which is detailed later, immediately suggests that this suppression of dissociation is associated with that *portion* of the initial vibrational wave packet which is cut by an intensity-dependent avoided crossing of the field-dressed molecular states, and is lifted by the increasing field to higher energies. Population is "shelved" [4] well away from the repulsive bond-softening [2] potential which opens the system to rapid dissociation. Although this phenomenon can be related to the intensity-sensitive *stabilized* bound states postulated by Bandrauk and Sink [5] we find the pulse actually forms a robust intensity-insensitive coherent

wave packet of adiabatic field-dressed states which we refer to as *population trapping*. In addition there is indirect experimental evidence that such transient bound states might be acting as final states in the photoionization of H_2 [6]. Although calculations are only presented for H_2^+ , we expect dissociative stabilization to be quite general. This trapping mechanism might even give insight to some aspects of ionization stabilization in atoms

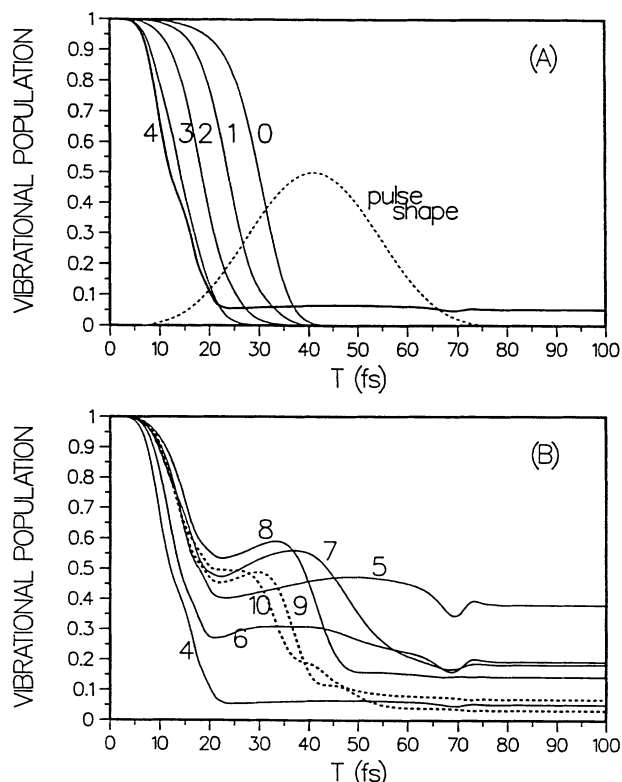


FIG. 1. Decay of the total bound state population ($v=1-18$) of H_2^+ ground state subjected to a 100-optical-cycle (83 fs) laser pulse [dotted line in (a)]. The wavelength is 248 nm and the peak intensity is 5×10^{14} W/cm². The numbers denote the initial vibrational level for each calculation. (b) Trapping occurs for $v \geq 4$.

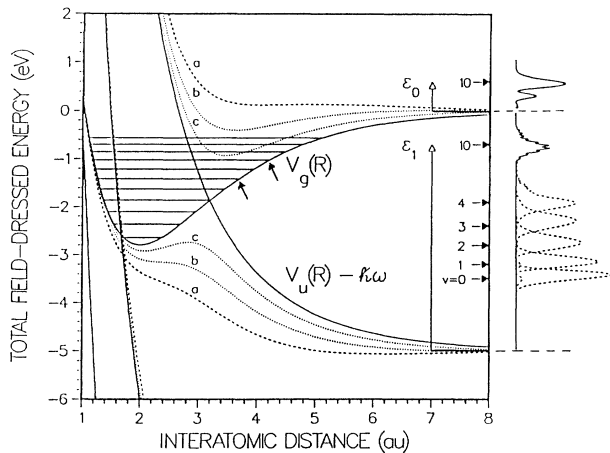


FIG. 2. Field-dressed $1\sigma_g$ and $2p\sigma_u$ states of H_2^+ , diabatic (full lines) and adiabatic (dashed lines). The photon energy is 5 eV ($\lambda=248$ nm) and the laser intensity (in units of 10^{14} W/cm 2) is (curve a) 5, (curve b) 2.5, and (curve c) 1. The fragment energy distribution is given on the right for initial levels $v=0-4$ (dashed lines) and $v=10$ (full line). ϵ_1 is the total asymptotic kinetic energy for bond-softening dissociation (σ_u , $n=1$ channel) and ϵ_0 for wave packet escape from the upper (σ_g , $n=0$) potential well. The two arrows pointing at the V_g potential show the position of the diabatic curve crossing for the wavelengths 355 nm (lower arrow) and 532 nm used in the calculations for Fig. 4.

[4,7].

For each initial v in Fig. 1 the curve shows the decay of the entire bound-state population ($v=0-18$) in the $1\sigma_g$ state as a function of time when subjected to a Gaussian-like $\sin^4(\pi t/2T_p)$ pulse which begins at $t=0$, peaks at $t=T_p$, and terminates at $t=2T_p$. These results are obtained by integrating the appropriate time-dependent Schrödinger equation using the short-time propagator and split operator algorithms [8]. Our calculations only include radiative coupling between the attractive ground state $1\sigma_g$ and the first totally repulsive $1p\sigma_u$ state which both asymptotically dissociate to $H^+ + H(1s)$. Recent multistate field-dressed variational calculations by Muller [9] which are fully converged and gauge invariant confirm that our two-state approximation should yield quite reliable results as long as we evaluate the radiative coupling in the dipole length approximation. At $R \approx 2$ a.u. the ionization potential (E_{IP}) of H_2^+ is 27 eV which justifies our neglect of competition with photoionization. In fact Muller's converged calculations for $\lambda=532$ nm, $I_p=10^{14}$ W/cm 2 were performed out to $R=6$ a.u. where $E_{IP} \approx 18$ eV without significant contributions from the ionization continuum. Certainly the asymptotic $H(1s)$ fragment with $E_{IP}=13.6$ eV might experience subsequent ionization at the intensities used in our calculations, but this will have little effect on the proton kinetic energy spectrum, or the trapping we are concerned with in this Letter. Furthermore the parameters chosen for our cal-

culations roughly conform to experimental conditions [2,10] where dissociation has been "observed." We also neglect rotational effects [3,8] and assume that the molecule is strongly aligned by the linearly polarized laser field as observed in experiments [2,10]. A more rigorous calculation would include an expansion in a reasonably complete set of rotational states. Unpublished calculations using time-independent Floquet methods already confirm that there is rapid alignment by optical pumping of rotational states in strong fields.

Although we explicitly solve the time-dependent Schrödinger equation for a given pulse shape, good insight into the process is obtained by studying the *adiabatic* field-dressed potentials [5] in Fig. 2. In time-independent or Floquet theory the wave function is expanded in a set of photon number states $|N-n\rangle$ centered around $N=18\pi V/c\hbar\omega$. Our calculations start with an attractive $V_g(R)$ potential defined by the lowest gerade state ψ_g , and a totally repulsive $V_u(R)$ potential defined by the lowest ungerade state ψ_u . The molecule-field channel state $\psi_g|N-n\rangle$ with $n=0$ defines the initial state of the system before any absorption ($n>0$) or stimulated emission ($n<0$) of photons from the laser field has occurred. In Fig. 2 the $n=0$ asymptote is scaled to zero and joins to the V_g potential which supports the initial vibrational state. The $n=1$ asymptote correlates with the $\psi_u|N-1\rangle$ channel and joins to the V_u potential, shifted by the loss of one photon due to absorption. These two channels can be viewed as *diabatic* field-dressed states for the combined molecule-field system.

In the weak field limit one-photon absorption will be dominated by the crossing of the two diabatic curves at $R \approx 3.2$ a.u. As the intensity increases with time the radiative interaction couples these two channels to the manifold of higher-order $\psi_u|N-n\rangle$ ($n=\text{odd}$) and $\psi_g|N-n\rangle$ ($n=\text{even}$) channels. In the strong field limit it is best to consider the *adiabatic* field-dressed states for the system. Using up to 41 channels the molecule-field Hamiltonian is diagonalized to generate the adiabatic curves a, b, and c in Fig. 2 corresponding to the intensities $I=(5, 2.5, \text{ and } 1) \times 10^{14}$ W/cm 2 , respectively. We can envision the system evolving from the uncoupled diabatic curves at $t=0$, progressively approaching the peaked adiabatic curve a at $t=T_p$, and then returning to the uncoupled diabatic curves as $t \rightarrow 2T_p$.

In Fig. 1 we see that the dissociation of $v=0-3$ is completed before the strongest adiabatic curve is reached. As I increases the adiabatic curve below the $R \approx 3.2$ a.u. crossing is repulsed downward and those vibrational states which predominantly lie to shorter distances suddenly become unbounded. This effect has been termed bond softening [2], and primarily leads to an $n=1$ kinetic energy peak in the photofragments, and severe repression of the $n \geq 2$ peaks which we referred to as above threshold dissociation (ATD) [3]. For weaker I_p these lower levels will experience a potential barrier which inhibits

the dissociation out of the $n=1$ channel and favors ATD.

The progressive lowering of the adiabatic bond-softening curve with intensity can be viewed as a *time-dependent ac Stark shift*. Since the shift first causes the adiabatic curve to drop below the $v=3$ state, an initial wave packet prepared in this state will experience the most rapid dissociation to the $n=1$ channel in the leading edge of the pulse. In Fig. 2 this can be viewed as a "projection" of the initial wave packet onto the appropriate adiabatic potential and yields the asymptotic distribution of fragment kinetic energies ϵ_1 for $v=3$ as shown to the right of the figure. The lower v require more severe shifting and yield lower kinetic energy peaks. This shifting effect would be observed in the distribution of proton kinetic energies $\epsilon^+ = \epsilon_1/2$ originating from the dissociation of H_2^+ in Eq. (1).

Turning to the $v=4$ state we begin to see a qualitative change in behavior in Fig. 1. The wave packet initially decays more rapidly than $v=3$, but then, starting at $t \approx 20$ fs about 5% of the bound-state population persists until the pulse is complete. The corresponding integrated probability of finding fragmentation of the $v=4$ state in the ϵ_1 peak near 3.0 eV is now only 0.944. Interestingly an interference pattern now appears on the high-energy side of the peak which is due to interfering continuum wave packets originating at the leading and trailing edge of the pulse. Equally interesting is the appearance of a miniscule amount (0.4%) of almost zero-kinetic-energy fragments which can be associated with fragmentation out of the $n=0$ channel with all its asymptotic amplitude associated with the ψ_g state. These three new features (population trapping, interferences, and $n=0$ dissociation) become significantly enhanced with higher initial v .

What we can surmise is that as the pulse rises a dominant (94%) portion of the initial wave packet is "pushed" down on the repulsive bond-softening potential which falls below the diabatic crossing, and this gives rise to the $n=1$ kinetic energy peak, as for the $v=0-3$ states. The small portion (5%) of the wave packet that lies above the diabatic crossing at $R \approx 3.2$ a.u., and to the right of the $V_u - \hbar\omega$ intersection is trapped and pushed up by the rising adiabatic potential, and effectively escapes from the bond-softening effect. For high enough intensities, such as for the $I = 5 \times 10^{14}$ W/cm² peak in Fig. 2, the upper adiabatic curve actually lies above the $n=0$ asymptote and pushes a portion of the trapped wave packet above the threshold. This is shown schematically for $v=10$ in Fig. 2 and explains the low-kinetic-energy fragments in Fig. 3. Depending on the pulse time, some of the trapped population can slowly escape to large distances before it once again falls below the threshold due to the subsequent collapse of the adiabatic potentials. Finally, as the upper curve becomes more diabatic at the trailing edge of the pulse some of the trapped amplitude again feeds flux into the bond-softening channel. This is separated from the leading-edge continuum wave packet

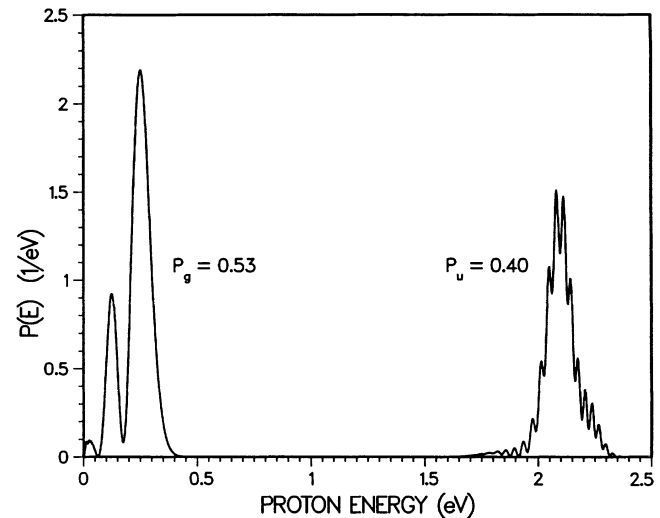


FIG. 3. Proton energy distribution for $H_2^+(v=10)$ dissociation by a 83-fs laser pulse with $\lambda=248$ nm and $I_p=5 \times 10^{14}$ W/cm². P_g is the integrated probability for $(\sigma_g, n=0)$ dissociation; P_u , for $(\sigma_u, n=1)$ dissociation. The missing population $1 - (P_g + P_u) = 0.07$ is trapped in bound states.

by approximately $\Delta t \approx T_p$ and qualitatively explains the spacing of the interference pattern in Fig. 3. An exact measure of Δt can be extracted from the calculated wave packet at the conclusion of the pulse, and conforms perfectly to the spacing $\Delta\epsilon_1 = \hbar/\Delta t$ of the oscillations in the $n=1$ peaks.

Figure 4 shows how the stabilization effect varies with the initial vibrational level and the pulse duration for three different wavelengths and intensities. The intensity is most severe for $\lambda=248$ nm and the $v=0$ to 3 levels are completely dissociated. The weaker intensities and higher position of the curve crossings for the other wavelengths (see arrows in Fig. 2) introduce tunneling in the bond-softening potential which suppresses the dissociation of the lower levels. However, as v increases further all the λ exhibit increased trapping in the bound states, beginning with the first vibrational level above the diabatic crossing, namely, $v=4, 6,$ and 8 for $\lambda=248, 355,$ and 532 nm, respectively. Shortening T_p and I_p and v fixed also increases trapping, mostly at the expense of decreased $n=0$ dissociation. Although the trapped wave packet is pushed above the $n=0$ threshold to the same extent by the peak adiabatic potential, it has only half the time to escape into the continuum before the pulse collapses the potential and traps molecules in high- v states once again.

Only the total population of molecules bound in any of the $v=0-18$ vibrational levels supported by the ground state is shown in Fig. 1. The exact distribution of population can be widely distributed among these states, with a strong bias towards leaving the molecule in the higher levels, even up to $v=18$. The details of these distributions will undoubtedly be a sensitive function of rotational state as well, and a more thorough analysis will be de-

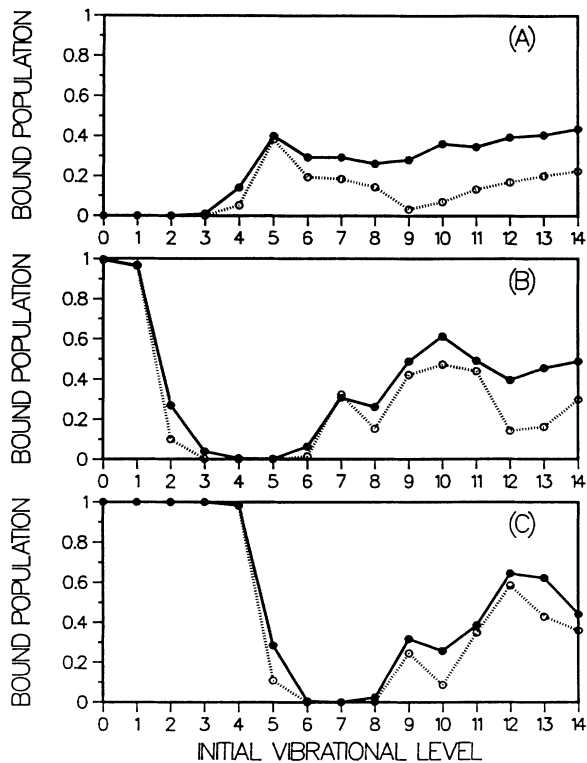


FIG. 4. Total bound-state population at the end of the laser pulse of 50 (solid lines) or 100 (dotted lines) optical cycles, as a function of initial vibrational level. (a) $\lambda=248$ nm, $I=5 \times 10^{14}$ W/cm² (100 cycles=83 fs). (b) $\lambda=355$ nm, $I=1 \times 10^{14}$ W/cm² (100 cycles=118 fs). (c) $\lambda=532$ nm, $I=2.5 \times 10^{13}$ W/cm² (100 cycles=177 fs).

ferred until these more complete J -dependent calculations are completed. However, the present results are consistent with the proposed trapping mechanism.

The experimental demonstration of trapping requires the preparation of H_2^+ in excited vibrational levels ($v > 5$) which is currently achieved in resonance enhanced multiphoton ionization experiments [2,6,10] in the range of wavelengths employed in our calculations. It would be difficult, as in the case of suppression of atomic

ionization [4], to find a direct signature of suppressed dissociation, but indirect evidence might already be seen in some experiments, on H_2 or other molecules [6,11]. The results suggest that temporary bound states in the upper field-induced potential well (Fig. 2) might be acting as final states in the photoionization of the neutral molecule. Although still indirect, the detection of very slow fragments due to partial escape of the trapped wave packet from the upper adiabatic well could be another signature of the trapping mechanism.

We thank R. W. Heather for his assistance with the time-dependent codes, and H. G. Muller for his generosity in sharing his results with us. This research was supported in part by a NATO Research Grant.

- [1] P. Lambropoulos, Phys. Rev. Lett. **55**, 2141 (1985).
- [2] P. H. Bucksbaum, A. Zavriyev, H. G. Muller, and D. W. Schumacher, Phys. Rev. Lett. **64**, 1883 (1990); A. Zavriyev, P. H. Bucksbaum, H. G. Muller, and D. W. Schumacher, Phys. Rev. A **42**, 5500 (1990).
- [3] A. Giusti-Suzor, X. He, O. Atabek, and F. H. Mies, Phys. Rev. Lett. **64**, 515 (1990).
- [4] R. R. Jones and P. H. Bucksbaum, Phys. Rev. Lett. **67**, 3215 (1991).
- [5] A. D. Bandrauk and M. L. Sink, J. Chem. Phys. **74**, 1110 (1981); J. Phys. Chem. **87**, 5098 (1983).
- [6] S. W. Allendorf, and A. Szöke, Phys. Rev. A **44**, 518 (1991).
- [7] M. V. Fedorov and M. Y. Ivanov, J. Opt. Soc. Am. B **7**, 569 (1990); M. Pont and M. Gavrilla, Phys. Rev. Lett. **65**, 2362 (1990); K. Burnett, P. L. Knight, B. R. M. Piraux, and V. C. Reed, Phys. Rev. Lett. **66**, 301 (1991).
- [8] R. W. Heather, Comput. Phys. Commun. **63**, 446 (1991); R. W. Heather and F. H. Mies, Phys. Rev. A **44**, 7650 (1991).
- [9] H. G. Muller, in Proceedings of Coherence Phenomena in Atoms and Molecules in Laser Fields, NATO Advanced Research Workshop, Hamilton, Ontario Canada, 1991 (to be published).
- [10] B. Yang, M. Saeed, L. F. DiMauro, A. Zavriyev, and P. H. Bucksbaum, Phys. Rev. A **44**, R1458 (1991).
- [11] J. E. Decker, G. Xu, and S. L. Chin, J. Phys. B **24**, L281 (1991).